Interface Induced Uniaxial Magnetic Anisotropy in Amorphous CoFeB Films on AlGaAs(001)

A. T. Hindmarch,[1,*] C. J. Kinane,[1] M. MacKenzie,[2] J. N. Chapman,[2] M. Henini,[3] D. Taylor,[3] D. A. Arena,[4] J. Dvorak,[5] B. J. Hickey,[1] and C. H. Marrows[1]

[1]*School of Physics & Astronomy, University of Leeds, Leeds, LS2 9JT United Kingdom*
[2]*Department of Physics & Astronomy, University of Glasgow, Glasgow, G12 8QQ United Kingdom*
[3]*School of Physics & Astronomy, University of Nottingham, Nottingham, NG7 2RD United Kingdom*
[4]*National Synchrotron Light Source, Brookhaven National Laboratory, Upton, New York 11973, USA*
[5]*Department of Physics, Montana State University, Bozeman, Montana 59717, USA*

(Received 17 September 2007; published 17 March 2008)

We demonstrate an isolated magnetic interface anisotropy in amorphous CoFeB films on (Al)GaAs(001), similar to that in epitaxial films but without a magnetocrystalline anisotropy term. The direction of the easy axis corresponds to that due to the interfacial interaction proposed for epitaxial films. We show that the anisotropy is determined by the relative orbital component of the atomic magnetic moments. Charge transfer is ruled out as the origin of the interface anisotropy, and it is postulated that the spin-orbit interaction in the semiconductor is crucial in determining the magnetic anisotropy.

DOI: 10.1103/PhysRevLett.100.117201 PACS numbers: 75.30.Gw, 75.50.Bb, 75.70.−i

Magnetic anisotropies in epitaxial ferromagnetic (FM) films on III–V semiconductors (SC), a prototypical system for spintronics, exhibit a variety of interesting and surprising phenomena [1–3]. Thin molecular beam epitaxy (MBE)-grown body-centered cubic (bcc) FM films on III–V(001) display an interface induced uniaxial magnetic anisotropy (UMA) with easy-axis (EA) along [110], the origin of which is suggested as being due to an interfacial, e.g., Fe-As, bonding interaction [1,4]. However, the true origin of this UMA is partially obscured as when it is combined with the cubic magnetocrystalline anisotropy due to the crystal structure of the epitaxial film, having fourfold symmetry with EA oriented along the {100} directions, complex magnetization reversal can result [2]. Proper understanding of this interface anisotropy remains one of the unanswered questions in modern magnetism, and is of crucial importance in spintronics.

To gain insight into the origins of the UMA in III–V(001)/FM one could, in principle, isolate it by removing the magnetocrystalline anisotropy contribution. This may be achieved by employing an amorphous FM, i.e., one having no long-range crystal symmetry. If the same interfacial interaction arises then a weak UMA with EA along [110] should be observed, with no cubic anisotropy present; the origin of the UMA would then be more easily accessible experimentally. In this Letter we report such an approach, using an amorphous $Co_{0.4}Fe_{0.4}B_{0.2}$ alloy in (Al)GaAs(001)/FM heterostructures in order to access the interface induced UMA alone.

Amorphous FM may be produced by alloying metalloid into the FM matrix: addition of ~20% metalloid (in this case B) in the FM transition metal (TM) alloy (here CoFe) only slightly reduces the Curie temperature and saturation magnetization [5], while destroying crystallinity [6]. Such CoFeB alloys have recently proven successful for spintronics applications [5,7–9]. However, only recently has the integration of amorphous CoFeB films into SC/FM spintronic devices begun to be investigated [10].

GaAs/AlGaAs heterostructures were grown by standard III–V MBE onto p^+-GaAs(001) wafers. The heterostructures consisted of p-AlGaAs/GaAs/n-AlGaAs quantum-well LEDs, one of which had an i-GaAs[50 Å] "tunnel barrier" interface layer while the other had a n^+-AlGaAs[150 Å] "Schottky" interface. These structures will henceforth be referred to, respectively, as either AlGaAs/GaAs or AlGaAs samples, where AlGaAs here represents $Al_{0.3}Ga_{0.7}As$. The structures are similar to those in Ref. [11] and were capped with arsenic to prevent oxidation on removal from the MBE chamber.

Metallic films were deposited by dc magnetron sputtering in a separate, custom built, vacuum chamber having a base pressure of $\sim 2 \times 10^{-8}$ Torr. The structures were heated to ~500 °C for 1 h under vacuum to remove the As capping layers. After cooling to 45 °C under vacuum, metal films of CoFeB[35 Å]/Ta[25 Å] were deposited. An in-plane magnetic field of $H_{\mathrm{Dep}} \sim 150$ Oe was applied parallel to one of the {110} directions during deposition and a $Co_{0.4}Fe_{0.4}B_{0.2}$ alloy sputter target was used. Magnetic measurements were made by longitudinal magneto-optical Kerr effect (MOKE) using a HeNe laser with spot-diameter ~0.5 mm, and cross-sectional high resolution transmission electron microscopy (HRTEM) was performed using a FEI Tecnai F20 transmission electron microscope. Soft x-ray absorption spectroscopy (SXAS) and magnetic circular dichroism (SXMCD) measurements were performed at the U4B beam line at the NSLS, Brookhaven. The circular polarization of the beam was set to 90% and the beam was incident at 45° to the sample normal. A saturating magnetic field was applied in the plane of the films and the photoexcited electron yield was collected perpendicular to the beam direction. Reversing the sample magnetization is equivalent to switching the

photon helicity σ, allowing it to couple either to majority or minority spin. This produces parallel (I^+) and antiparallel (I^-) absorption spectra from which an SXMCD difference spectrum, $I^+ - I^-$, may be derived [12].

Figure 1 shows MOKE hysteresis loops for CoFeB films on AlGaAs/GaAs and AlGaAs epilayers. The magnetic field during measurement is applied either parallel or perpendicular to the deposition field. One immediately notices a significant UMA in both films and that the uniaxial EA are perpendicular to the applied deposition field direction. Polycrystalline and amorphous FM films deposited in an applied magnetic field typically show a deposition field induced UMA with EA in the direction of the applied deposition field [13]: this is the case for $Co_{0.4}Fe_{0.4}B_{0.2}$ films deposited on Si wafers. However, this is not observed in our CoFeB films on AlGaAs and AlGaAs/GaAs; the UMA does not originate from the field applied during deposition. For the structure with GaAs interface, an entirely reversible magnetization reversal by coherent rotation is observed along the hard axis (HA), whereas for the sample without GaAs HA reversal takes place partially by domain wall motion. In this film the HA saturation field is reduced, indicating that stronger UMA is present in the structure with GaAs interface.

Here, we show that the UMA in amorphous CoFeB films is consistent with the III–V(001)/FM interface interaction in epitaxial systems. Having successfully removed the cubic magnetocrystalline anisotropy term we demonstrate the mechanism by which the UMA arises in FM films on III–V(001).

HRTEM images of the structures are shown in Fig. 2: the CoFeB films appear amorphous, although as in Ref. [8] interfacial crystallinity at the SC/FM interface may not be ruled out. The cross sections are viewed along the [110] and [1$\bar{1}$0] directions. Both samples show clean SC/FM interfaces comparable to those observed in MBE-grown AlGaAs/Fe [14] and it is clear that the sputtered films closely follow the epilayer surface morphology. Corrugation of the SC surface is apparent for the AlGaAs/GaAs structure shown in Figs. 2(a) and 2(b), having amplitude $\Delta \sim 25$ Å and period $\xi \sim 250$ Å along the EA while being flat along the HA. Lower magnification scanning TEM images (not shown) of films on AlGaAs show a corrugation with similar Δ, and $\xi\sim$ several 1000 s of Å.

One may see that the differences in the observed HA reversal processes are related to the corrugation in the epilayer surfaces by comparing ξ to the domain wall thickness D. For a Néel-type domain wall, typically the case in thin films, this may be estimated from $D \simeq \pi(2A/K_U^{\mathrm{eff}})^{1/2}$ where K_U^{eff} is the effective uniaxial anisotropy constant (due to the lack of crystal symmetry $K_U^{\mathrm{eff}} = K_U/t$, K_U is the uniaxial interface anisotropy constant and t the film thickness) and A the exchange stiffness. Quantitative values for the uniaxial anisotropy constant may be obtained from fitting a Stoner-Wohlfarth model to the magnetization data in Fig. 1(a).

For a ferromagnet with UMA and magnetic field applied parallel to the HA, the magnetic free-energy density ε may be written as $\varepsilon = K_U^{\mathrm{eff}}\sin^2(\theta_{\mathrm{HM}}) - \mathrm{HM}_S\cos(\theta_{\mathrm{HM}})$, where θ_{HM} is the angle between magnetization and applied field H, and M_S is the saturation magnetization. The Stoner-Wohlfarth model is valid for single-domain reversible magnetization rotation which is the case for AlGaAs/GaAs/CoFeB: from the fit in Fig. 1(a) we obtain $K_U^{\mathrm{eff}} = 29$ kJ/m^3, significantly weaker than the $\sim$67 kJ/m^3 for similarly thick epitaxial Fe films [2] but comparable with that in our epitaxial sputtered $Co_{0.7}Fe_{0.3}$. Taking this anisotropy constant and the exchange stiffness $A \sim 28 \times 10^{-12}$ J/m^3 [15], we obtain a domain wall width $D \sim 1500$ Å for CoFeB on AlGaAs/GaAs. It is reasonable

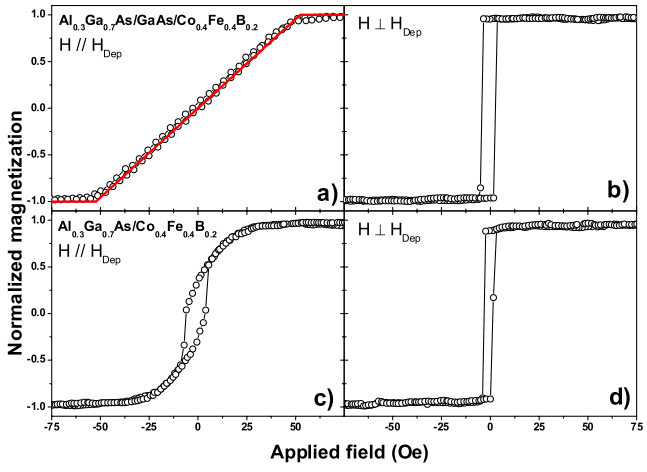

FIG. 1 (color online). Room temperature MOKE hysteresis loops of AlGaAs/GaAs/CoFeB[35 Å], (a),(b), and AlGaAs/CoFeB[35 Å], (c),(d), contacts. The field is applied parallel or perpendicular to the deposition field, as indicated. The solid line in frame (a) is a fit using the Stoner-Wohlfarth model described in the main text.

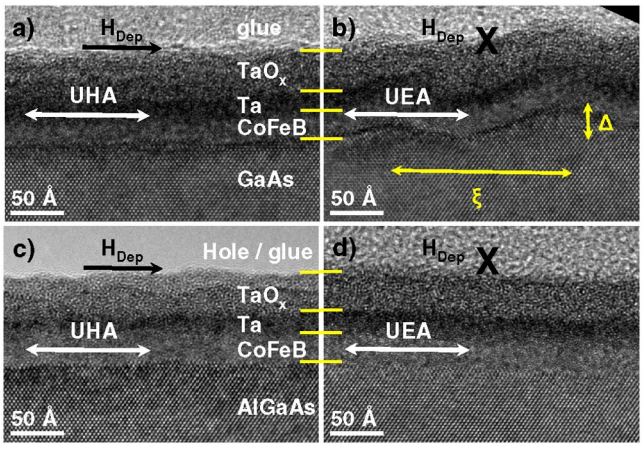

FIG. 2 (color online). Cross-sectional HRTEM micrographs of the same AlGaAs/GaAs/CoFeB, (a),(b), and AlGaAs/CoFeB, (c),(d), contacts. The growth field direction and uniaxial magnetic anisotropy axes are indicated in each frame. The corrugation period ξ and amplitude Δ are indicated in frame (b).

that the substrate surface corrugation is able to influence domain walls for CoFeB on AlGaAs epilayers where $D \sim \xi$, but not for AlGaAs/GaAs where $D \gg \xi$. The substrate surface corrugation observed by HRTEM explains the difference in HA magnetization reversal mechanism.

It has recently been suggested that isotropic substrate roughness can act to decrease the effective UMA with increasing Δ/ξ ratio due to surface magnetic "charges" [16]. There is no decrease in the HA saturation field as the reduction in effective UMA is due to increased free-energy for magnetization aligned nominally along the EA; anisotropic roughness alone would act to induce an EA along the corrugation in the absence of any interface interaction [17]. The surface corrugation could also influence the UMA direction through magnetostriction [18]. However, as ξ is much smaller than the laser spot diameter, our MOKE measurements represent an average over many periods of both tensile and compressive strain; for either positive or negative magnetostriction one would expect to observe mixed hard- and easy-axis behavior were this the case. The corrugation propagates from deep within the III–V heterostructure; it is present prior to the growth of the CoFeB film and hence is unlikely to induce significant strain. The UMA has EA oriented along an in-plane {110}, consistent with that observed in epitaxial systems. Similar $Co_{0.7}Fe_{0.3}$ films grown on substrates cut from the same wafer also exhibit this UMA, combined with the cubic magnetocrystalline term: these epitaxial films show none of the hysteresis features characteristic of films grown on vicinal substrates [19]. Thus the most compelling explanation for the UMA in these amorphous CoFeB films is the interfacial interaction observed in epitaxial III–V/bcc FM [2].

Regarding the difference in HA saturation field, it is well known that orbital angular momentum plays a dominant role in determining the strength of magnetocrystalline anisotropy, even in transition metals [20]. To demonstrate that the different SC interface layers influence the UMA through the orbital component of the atomic magnetic moments, we have performed SXMCD measurements on our CoFeB films. Using this technique one is able to extract the atomic magnetic moments (strictly, per valence hole), or the orbital and spin components thereof, with element specificity [21,22]. In a crystalline FM film the orbital moment may contribute both to the uniaxial and cubic magnetocrystalline anisotropies; only by using an amorphous FM are we able to disentangle its influence on the UMA alone.

SXMCD spectra around the Co and Fe L_{II} and L_{III} absorption edges for CoFeB on AlGaAs/GaAs and AlGaAs epilayers are shown in Fig. 3. The measurements are taken with the in-plane HA of the films aligned parallel to the 75 Oe applied field. For both structures a clear dichroic signal is observed at each of the four absorption edges. The integrated white-line SXAS intensities indicate that there is no significant difference in interface bonding charge transfer (BCT) between AlGaAs and AlGaAs/GaAs structures [4] at either Co or Fe sites. This demonstrates that the roughness profiles, Fig. 2, do not influence the electronic structure of the CoFeB films, e.g., via bonding coordination. Quantitative analysis of SXMCD data is nontrivial as the result is strongly dependent on subtle details of the SXAS background subtraction; we do not give quantitative measures of either spin, orbital or total moments as these also depend on the (unknown) d-band hole density in CoFeB. The qualitative changes in the orbital to spin moment ratios are robust to the background subtraction applied to the SXAS data.

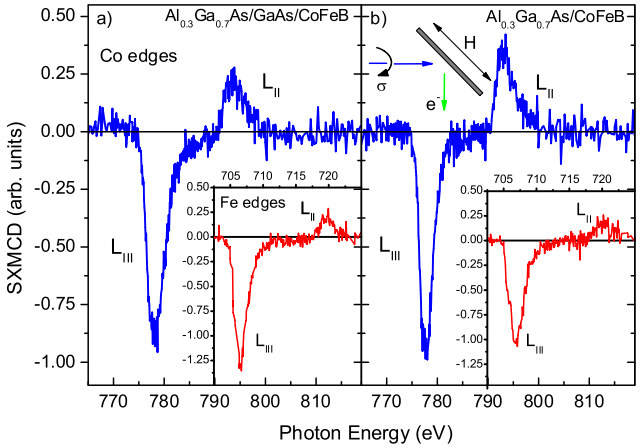

FIG. 3 (color online). SXMCD difference spectra across the Co (main) and Fe (inset) L_{II} and L_{III} absorption edges for the same CoFeB [35 Å] films deposited on (a) AlGaAs/GaAs or (b) AlGaAs epilayers. For both elements, the insertion of a GaAs interface layer results in an increase in the ratio of orbital to spin magnetic moments, increasing the relative L_{III}:L_{II} dichroism. The upper inset to frame (b) shows the SXMCD measurement geometry schematically.

Concentrating first on the Co absorption edges, shown in the main frames of Fig. 3, we see that the CoFeB film on AlGaAs/GaAs epilayer shows a significantly reduced SXMCD signal around the L_{II} absorption edge in comparison with the film on AlGaAs. Recalling the x-ray magnetic circular dichroism sum rules [21,22] used to calculate the film averaged orbital (m_{orb}), spin (m_{spin}), and total magnetic moments, this suggests that the GaAs interface layer results in a partial quenching of the Co spin moment. Such quenching has been observed in epitaxial Co films on GaAs(110) [23]. Applying the sum-rules using the method of Chen *et al.* [12], we find that m_{orb}/m_{spin} for Co sites increases from 0.19 for CoFeB on AlGaAs epilayer to 0.38 for AlGaAs/GaAs, in both cases enhanced over the bulk elemental values [12,22].

Turning our attention to the Fe absorption edges shown in the insets to Fig. 3, we again see an enhancement in m_{orb}/m_{spin} with the GaAs interface layer. In this case the L_{III} dichroism is enhanced for the film on AlGaAs/GaAs while the L_{II} dichroism is similar for both samples, suggesting that the enhancement in m_{orb}/m_{spin} for Fe sites is due to an increase in the orbital moment rather than the

suppression of the spin moment seen from the Co dichroism. Enhancement in the orbital to spin magnetic moments has also previously been observed by SXMCD measurements on thin epitaxial Fe/GaAs(001) [24]. Applying the sum-rules as before results in Fe $m_{\mathrm{orb}}/m_{\mathrm{spin}}$ increasing for the substrate with GaAs interface layer. The Fe $m_{\mathrm{orb}}/m_{\mathrm{spin}}$ ratios are 0.34 for AlGaAs epilayer and 0.45 for AlGaAs/GaAs, again slightly enhanced over elemental values [24]. The increase in Co and Fe $m_{\mathrm{orb}}/m_{\mathrm{spin}}$ ratios observed in our SXMCD measurements corresponds with the enhancement in UMA for CoFeB on AlGaAs/GaAs over that on AlGaAs.

Variation in the orbital and spin moments cf. bulk elemental values could be explained by BCT due to bonding within the CoFeB alloy, although such BCT is expected to be minimal. BCT between Co and Fe sites in the disordered FeCo alloy system—considered here as an analog of CoFeB—is small [25], the same being true for BCT from boron to TM sites [26]. As the only chemical difference between the two structures is the interface layer onto which the CoFeB film is deposited, it appears that the SC/FM interface must in some way play a crucial role in determining the strength of the UMA through the relative orbital component of the magnetic moments associated with both Co and Fe sites. BCT also occurs due to interfacial bonding [4]; we point out that the interfacial As concentration is identical, as is any BCT due to the bonding interaction. Considering again the disordered FeCo alloy, the majority d band is filled and the minority d band at the Fermi energy has mainly Fe character [25]. Introducing a small transfer of charge should thus result in a change only in the spin moment associated with Fe sites with little change in Co moments, contradicting the results of our SXMCD measurements. It is not possible to reconcile our observations with SC-metal BCT; this is not the origin of the interfacial UMA.

Recently it has been demonstrated in Au/Co/Au trilayers displaying a temperature-driven spin-reorientation transition that the interface magnetic anisotropy and the anisotropy of the orbital magnetic moment in the Co layer may be significantly altered by the spin-orbit interaction in the adjacent Au layers [27]. For this to occur, both strong hybridization between Co and Au states, and the strong spin-orbit interaction in Au were shown to be required. We suggest that this mechanism may also be responsible for the interfacial UMA in III–V/FM systems: strong hybridization is clearly present between (Al)GaAs and CoFeB as demonstrated by BCT, and the spin-orbit parameter in, e.g., GaAs ($\sim$0.34 eV) is significantly stronger than that in Au ($\sim$0.006 eV). The spin-orbit parameter for AlGaAs is somewhere between that of GaAs and AlAs ($\sim$0.28 eV), which corresponds to the weaker UMA which we observe in CoFeB films on AlGaAs cf. GaAs interface.

In conclusion, we have successfully isolated the UMA induced at a III–V(001)/FM interface using thin amorphous CoFeB films sputter-deposited onto AlGaAs/GaAs and AlGaAs heterostructures. The uniaxial EA lies along one of the in-plane {110} directions, as in epitaxial systems. The stronger UMA for CoFeB on AlGaAs/GaAs cf. AlGaAs is shown, from SXMCD measurements at the Co and Fe L_{II} and L_{III} absorption edges, to be due to an enhancement in the relative orbital to spin magnetic moments associated with both Fe and Co sites. This enhancement cannot be explained due to the commonly assumed Fe-As BCT, ruling this out as the mechanism responsible for producing the interface anisotropy. We suggest that the interface interaction which produces the UMA in the FM overlayer is actually due to the spin-orbit interaction in the III–V semiconductor on which it is deposited.

The authors would like to acknowledge financial support from EPSRC, including via the "Spin@RT" consortium, and from the EU via Project No. NMP2-CT-2003-505587 "SFINx." We are grateful to BNL for the provision of NSLS beam time.

*a.t.hindmarch@leeds.ac.uk
http://www.stoner.leeds.ac.uk

[1] J. J. Krebs, B. T. Jonker, and G. A. Prinz, J. Appl. Phys. **61**, 2596 (1987).
[2] O. Thomas *et al.*, Phys. Rev. Lett. **90**, 017205 (2003).
[3] H. B. Zhao *et al.*, Phys. Rev. Lett. **95**, 137202 (2005).
[4] J. W. Freeland *et al.*, Phys. Rev. B **63**, 193301 (2001).
[5] Y. Luo *et al.*, Phys. Rev. B **72**, 014426 (2005).
[6] J. Hafner, M. Tegze, and C. Becker, Phys. Rev. B **49**, 285 (1994).
[7] D. X. Wang *et al.*, IEEE Trans. Magn. **40**, 2269 (2004).
[8] D. D. Djayaprawira *et al.*, Appl. Phys. Lett. **86**, 092502 (2005).
[9] A. T. Hindmarch *et al.*, J. Appl. Phys. **99**, 08K701 (2006).
[10] K. Sugiura *et al.*, Appl. Phys. Lett. **89**, 072110 (2006).
[11] A. T. Hindmarch *et al.*, J. Appl. Phys. **101**, 09D106 (2007).
[12] C. T. Chen *et al.*, Phys. Rev. Lett. **75**, 152 (1995).
[13] M. S. Blois, Jr., J. Appl. Phys. **26**, 975 (1955).
[14] T. J. Zega *et al.*, Phys. Rev. Lett. **96**, 196101 (2006).
[15] C. Bilzer *et al.*, J. Appl. Phys. **100**, 053903 (2006).
[16] C. A. F. Vaz, S. J. Steinmuller, and J. A. C. Bland, Phys. Rev. B **75**, 132402 (2007).
[17] R. D. McMichael *et al.*, J. Appl. Phys. **88**, 3561 (2000).
[18] R. J. Hicken and G. T. Rado, Phys. Rev. B **46**, 11688 (1992).
[19] A. F. Isakovic *et al.*, J. Appl. Phys. **89**, 6674 (2001).
[20] J. Trygg *et al.*, Phys. Rev. Lett. **75**, 2871 (1995).
[21] B. Thole *et al.*, Phys. Rev. Lett. **68**, 1943 (1992).
[22] P. Carra *et al.*, Phys. Rev. Lett. **70**, 694 (1993).
[23] M. Izquierdo *et al.*, Phys. Rev. Lett. **94**, 187601 (2005).
[24] J. S. Claydon *et al.*, Phys. Rev. Lett. **93**, 037206 (2004).
[25] A. Y. Liu and D. J. Singh, Phys. Rev. B **46**, 11145 (1992).
[26] A. Andrejczuk *et al.*, J. Phys. Condens. Matter **4**, 2735 (1992).
[27] C. Andersson *et al.*, Phys. Rev. Lett. **99**, 177207 (2007).